

Washington University School of Medicine

Digital Commons@Becker

---

2020-Current year OA Pubs

Open Access Publications

---

3-17-2023

## Imaging of brain structural and functional effects in people with human immunodeficiency virus

Erin E O'Connor  
*University of Maryland - Baltimore*

Edith V Sullivan  
*Stanford University*

Linda Chang  
*University of Maryland - Baltimore*

Dima A Hammoud  
*NIH Clinical Center*

Tony W Wilson  
*Boys Town National Research Hospital*

*See next page for additional authors*

Follow this and additional works at: [https://digitalcommons.wustl.edu/oa\\_4](https://digitalcommons.wustl.edu/oa_4)



Part of the [Medicine and Health Sciences Commons](#)

**Please let us know how this document benefits you.**

---

### Recommended Citation

O'Connor, Erin E; Sullivan, Edith V; Chang, Linda; Hammoud, Dima A; Wilson, Tony W; Ragin, Ann B; Meade, Christina S; Coughlin, Jennifer; and Ances, Beau M, "Imaging of brain structural and functional effects in people with human immunodeficiency virus." *Journal of infectious diseases*. 227, Supplement 1. S16 - S29. (2023).

[https://digitalcommons.wustl.edu/oa\\_4/3219](https://digitalcommons.wustl.edu/oa_4/3219)

This Open Access Publication is brought to you for free and open access by the Open Access Publications at Digital Commons@Becker. It has been accepted for inclusion in 2020-Current year OA Pubs by an authorized administrator of Digital Commons@Becker. For more information, please contact [vanam@wustl.edu](mailto:vanam@wustl.edu).

---

**Authors**

Erin E O'Connor, Edith V Sullivan, Linda Chang, Dima A Hammoud, Tony W Wilson, Ann B Ragin, Christina S Meade, Jennifer Coughlin, and Beau M Ances

# Imaging of Brain Structural and Functional Effects in People With Human Immunodeficiency Virus

Erin E. O'Connor,<sup>1,✉</sup> Edith V. Sullivan,<sup>2,3</sup> Linda Chang,<sup>1,4</sup> Dima A. Hammoud,<sup>5</sup> Tony W. Wilson,<sup>6</sup> Ann B. Ragin,<sup>7</sup> Christina S. Meade,<sup>8</sup> Jennifer Coughlin,<sup>9,a</sup> and Beau M. Ances<sup>10,a</sup>

<sup>1</sup>Department of Diagnostic Radiology & Nuclear Medicine, University of Maryland School of Medicine, Baltimore, Maryland, USA; <sup>2</sup>Department of Psychiatry and Behavioral Sciences, Stanford University School of Medicine, Stanford, California, USA; <sup>3</sup>Center for Health Sciences, SRI International, Menlo Park, California, USA; <sup>4</sup>Department of Neurology, Johns Hopkins University School of Medicine, Baltimore, Maryland, USA; <sup>5</sup>Center for Infectious Disease Imaging, Radiology and Imaging Sciences, NIH Clinical Center, Bethesda, Maryland, USA; <sup>6</sup>Institute for Human Neuroscience, Boys Town National Research Hospital, Boys Town, Nebraska, USA; <sup>7</sup>Department of Radiology, Feinberg School of Medicine, Northwestern University, Chicago, Illinois, USA; <sup>8</sup>Department of Psychiatry and Behavioral Sciences, Duke University School of Medicine, Durham, North Carolina, USA; <sup>9</sup>Department of Neurology, Washington University School of Medicine, St Louis, Missouri, USA; and <sup>10</sup>Department of Psychiatry and Behavioral Sciences, Johns Hopkins University School of Medicine, Baltimore, Maryland, USA

Before the introduction of antiretroviral therapy, human immunodeficiency virus (HIV) infection was often accompanied by central nervous system (CNS) opportunistic infections and HIV encephalopathy marked by profound structural and functional alterations detectable with neuroimaging. Treatment with antiretroviral therapy nearly eliminated CNS opportunistic infections, while neuropsychiatric impairment and peripheral nerve and organ damage have persisted among virally suppressed people with HIV (PWH), suggesting ongoing brain injury. Neuroimaging research must use methods sensitive for detecting subtle HIV-associated brain structural and functional abnormalities, while allowing for adjustments for potential confounders, such as age, sex, substance use, hepatitis C coinfection, cardiovascular risk, and others. Here, we review existing and emerging neuroimaging tools that demonstrated promise in detecting markers of HIV-associated brain pathology and explore strategies to study the impact of potential confounding factors on these brain measures. We emphasize neuroimaging approaches that may be used in parallel to gather complementary information, allowing efficient detection and interpretation of altered brain structure and function associated with suboptimal clinical outcomes among virally suppressed PWH. We examine the advantages of each imaging modality and systematic approaches in study design and analysis. We also consider advantages of combining experimental and statistical control techniques to improve sensitivity and specificity of biotype identification and explore the costs and benefits of aggregating data from multiple studies to achieve larger sample sizes, enabling use of emerging methods for combining and analyzing large, multifaceted data sets. Many of the topics addressed in this article were discussed at the National Institute of Mental Health meeting “Biotypes of CNS Complications in People Living with HIV,” held in October 2021, and are part of ongoing research initiatives to define the role of neuroimaging in emerging alternative approaches to identifying biotypes of CNS complications in PWH. An outcome of these considerations may be the development of a common neuroimaging protocol available for researchers to use in future studies examining neurological changes in the brains of PWH.

**Keywords.** MEG; MRI; PET; harmonization; neuroimaging; structure.

HIV invasion of the central nervous system (CNS) occurs within days after exposure [1]. The ensuing inflammatory cascade results in a transient aseptic meningitis or encephalitis that can lead to neuronal death in acute infection prior to the initiation of antiretroviral therapy (ART) [2]. This neuronal damage may be responsible for neuropsychological dysfunction in

virally suppressed people with HIV (PWH), also known as the “legacy effect.” In virally suppressed PWH, persistent inflammation in the CNS and CNS viral reservoirs may also contribute to neuropsychological dysfunction in the chronic phase of infection. While it remains difficult to assess these changes in the brain, neuroimaging provides a reliable and reproducible noninvasive *in vivo* method to measure and track changes in brain structure and function in PWH.

<sup>a</sup>J. C. and B. M. A. contributed equally to this work.

Correspondence: Erin E. O'Connor, MD, Department of Diagnostic Radiology & Nuclear Medicine / 22 S. Greene St., Baltimore MD 21201 ([erin.oconnor@umm.edu](mailto:erin.oconnor@umm.edu)).

The Journal of Infectious Diseases® 2023;227(S1):S16–29

© The Author(s) 2023. Published by Oxford University Press on behalf of Infectious Diseases Society of America.

This is an Open Access article distributed under the terms of the Creative Commons Attribution-NonCommercial-NoDerivs licence (<https://creativecommons.org/licenses/by-nc-nd/4.0/>), which permits non-commercial reproduction and distribution of the work, in any medium, provided the original work is not altered or transformed in any way, and that the work is properly cited. For commercial re-use, please contact [journals.permissions@oup.com](mailto:journals.permissions@oup.com)  
<https://doi.org/10.1093/infdis/jiac387>

## STRUCTURAL BRAIN IMAGING

### Macrostructural Magnetic Resonance Imaging Techniques

Structural magnetic resonance (MR) imaging has been used to measure macrostructural differences in PWH since the early days of the HIV epidemic. Macrostructural neuroimaging using conventional T1-weighted MR imaging provides measures of whole-brain or regional gray matter (GM), white matter

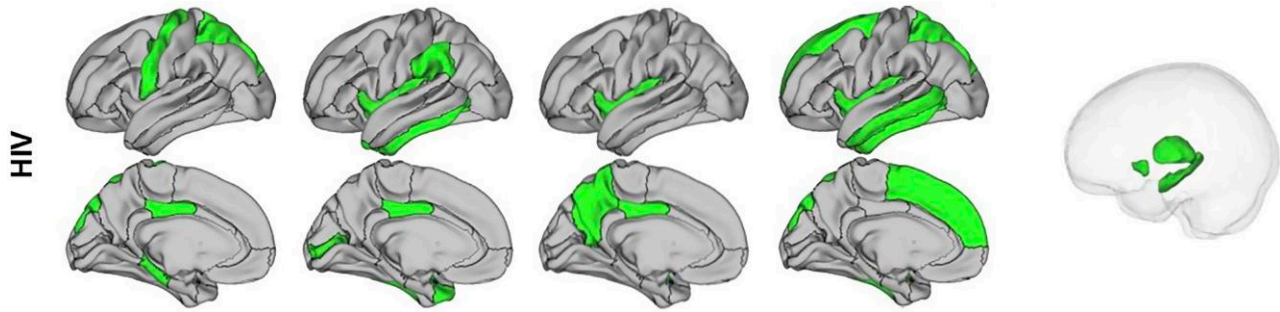


**Figure 1.** A novel machine learning approach identified a human immunodeficiency virus (HIV) diagnostically specific pattern of cortical and subcortical volume, surface area, mean curvature, or thickness deficits in the regions, noted in green. The top 4 sagittal images mark the precentral motor strip, superior parietal cortex, pars triangularis, insula, inferior and middle temporal gyri, and superior frontal cortex. The bottom 4 sagittal images mark the caudal anterior cingulum, parahippocampal gyrus, occipital cortex, pericalcarine, fusiform, temporal pole, precuneus, and medial frontal cortex. The leftward-facing sagittal image marks the thalamus, hippocampus, and accumbens. The pattern of cortical and subcortical regions specific to HIV emerged from a novel machine learning approach that differentiated HIV from other diagnoses (alcohol use disorder, HIV plus alcohol use disorder, and controls). (This image is a portion of figure published elsewhere [3, p 4], reprinted with permission from Elsevier.)

(WM), and cerebrospinal fluid. GM measures include volume, thickness, and surface morphometry [3, 4]. Automated segmentation of brain structures can be performed using brain atlases in standardized anatomical spaces [5].

The effects of HIV have diminished with time in all CNS tissue compartments, likely related to widespread use of ART [6, 7]. Nevertheless, brain structural differences can still be detected in chronically infected, virally suppressed PWH with voxel-wise volumetric approaches [8–10], cortical surface shape analysis [11–14], and cortical thickness estimation approaches [8, 15]. Yet to be determined is whether aging interacts with treated HIV infection to diminish improvement in pretreatment structural changes conferred by ART.

GM volume deficits in virally suppressed PWH relative to uninfected controls have been reported in frontal and parietal cortices [16], the transitional cortex of the insula and cingulum [16], and subcortical structures comprising basal ganglia, thalamus, and hippocampus [3, 16–18] (Figure 1). The smaller hippocampus, thalamus, and putamen and enlarged ventricles were associated with current CD4<sup>+</sup> cell counts, viral load, and ART status [19]. Cortical and subcortical GM volume deficits were more pronounced in those with AIDS-defining illness history [20].

WM structures exhibiting volume deficits in PWH included centrum semiovale and corpus callosum [21, 22]. Stratification by clinical symptoms and cognitive performance as unimpaired, asymptomatic neurocognitive impairment, mild neurocognitive disorder, or HIV-associated dementia revealed the following: (1) smaller medial orbitofrontal WM volume in asymptomatic neurocognitive impairment; (2) enlarged lateral ventricles and small volumes of frontal, cingulate, and parietal WM occurring in mild neurocognitive disorder; and (3) smaller volumes correlated with CD4<sup>+</sup>/CD8<sup>+</sup> cell count ratios [23, 24]. Lower CD4<sup>+</sup> cell count nadir and detectable HIV RNA were associated with smaller total WM volumes [25].

The greater presence of WM hyperintensities, often quantified with fluid-attenuated inversion recovery (FLAIR) imaging, occurs with older age, longer HIV infection duration, and CD4<sup>+</sup> cell counts <500/mL [26, 27]. There is also evidence that cerebrovascular risk factors contribute more than HIV-seropositive status to the development of WM lesions in PWH [28, 29].

The noninvasive nature of MR imaging enables safe, longitudinal studies in PWH [7, 30]. Some longitudinal studies of virally suppressed PWH provide confirmation of similar cross-sectional findings across the aging spectrum [13], including accelerated volume loss associated with older age, higher plasma viral loads, lower CD4<sup>+</sup> cell counts, and cognitive deficits [21, 31–33]. Such longitudinal work also showed HIV-by-age interactions in frontal and posterior parietal volumes in PWH [16]. Controversy remains, however, regarding how chronic HIV shapes brain aging [34], with some studies finding no differences in rates of change of structural (or other neuroimaging) measures over approximately 2 years [8, 35].

Structural MR imaging findings in PWH can help identify CNS correlates of clinical symptoms. For example, objective signs of neuropathy in virally suppressed PWH are correlated with smaller cerebellar vermis volumes, while subjective symptoms of neuropathy were associated with smaller precuneus volumes [36]. Furthermore, lower pontocerebellar volumes in PWH were correlated with impaired postural stability and psychomotor speed [37].

#### Microstructural MR Imaging Techniques

MR imaging diffusion tensor imaging (DTI) of WM microstructure yields measures of fiber organization (fractional anisotropy [FA]) and unrestricted water motility (mean diffusivity [MD]). Many studies have found alterations in FA and in MD in PWH, particularly in subcortical brain regions, such as the basal ganglia and corpus callosum [30, 38–40]

Abnormalities in DTI parameters suggest compromised tissue and HIV-associated neuroinflammation. Diffusion basis spectrum imaging, using a tensor model sensitive to the effects of cellularity, found higher cellularity in aviremic PWH, which also suggests persistent inflammation [41]. Diffusion alterations in PWH correlated with elevated levels of inflammatory biomarkers, such as cytokines (eg, tumor necrosis factor  $\alpha$  and interleukin 6), chemokines (eg, monocyte chemoattractant protein 1) and metalloproteinases, even in virally suppressed PWH [30, 41–44]. Markers of inflammation also were identified as discriminating features in machine learning models of HIV-induced brain injury, as quantified with diffusion and brain volume measures [30].

Cross-sectional studies found associations between clinical indices and diffusion measures. Higher FA and lower MD were associated with high CNS penetrance of HIV treatment, higher CD4<sup>+</sup> cell counts, and greater recovery from the CD4<sup>+</sup> cell count nadir [45, 46]. Furthermore, a greater number of years with CD4<sup>+</sup> cell counts <500/ $\mu$ L was associated with lower FA and higher MD in the projection, association, and callosal fiber systems [47]. A controlled study using DTI fiber tracking found higher MD in posterior corpus callosum, internal and external capsules, and superior cingulate bundles in PWH than in controls. Among the PWH, diffusivity differences from the control group in the posterior corpus callosum, fornix, and superior cingulate bundle were greatest in those with an AIDS-defining event [48].

## FUNCTIONAL MR IMAGING

Functional imaging studies, including blood oxygen level-dependent (BOLD)–contrast functional MR imaging and perfusion MR imaging, are used to assess neuronal functioning that complements structural neuroimaging techniques. BOLD-contrast functional MR imaging can evaluate brain function at rest or during a task by measuring the MR imaging signal changes associated with varying levels of oxygenated versus deoxygenated hemoglobin. Images obtained with resting-state functional MR (rsfMR) imaging are readily acquired and amenable to myriad analysis approaches. The brain at rest has low-frequency spontaneous fluctuations that exhibit coherent activity across spatially distinct networks. These correlations are used to estimate interregional functional connectivity.

PWH show subtly altered functional connectivity in some networks regardless of age [49]. rsfMR imaging that evaluated PWH in various stages of HIV-associated neurocognitive disorder (HAND) found altered connectivity in canonical brain networks, including the salience, default mode, and executive networks [50]. Network disruptions were detected even in those with acute HIV infection [51]. By contrast, task-related functional MR imaging requires participants to perform

specific tasks or view images that can elicit regional brain activity change. PWH typically showed lower task-induced activation within the normal networks but greater activation in reserve brain regions with the more demanding tasks and greater attentional load [52–59] or risk-taking behaviors [60–62]. These studies detected neural abnormalities with increasing cognitive demand in PWH. While task functional MR imaging is more challenging to implement in routine clinical care, it is generally associated with large changes in BOLD-contrast, and therefore may be more sensitive than rsfMR imaging for monitoring treatment or intervention effects [63].

Other functional imaging techniques, such as dynamic susceptibility contrast and arterial spin labeling (ASL), have been used more rarely to study brain perfusion in PWH. Dynamic susceptibility contrast showed relative changes in regional perfusion in PWH but requires a gadolinium contrast agent [64]. ASL is easier to acquire since it does not require gadolinium or radioactive tracers; instead, it assesses regional cerebral blood flow with radiofrequency pulses to label water molecules in the cerebral vasculature. Lower perfusion is seen in the lentiform nuclei in both acute and chronic phases of HIV infection [65], whereas cortical perfusion findings vary [65, 66]. Age, viral load, and treatment status can influence perfusion [66, 67].

## PROTON MR SPECTROSCOPY

Proton MR spectroscopy noninvasively probes neuropathology by measuring levels of metabolites that reflect neuronal health and integrity or neuroinflammation. By reliably detecting chronic HIV infection effects, proton MR spectroscopy may be useful for assessing the pathophysiology associated with cognitive and sensorimotor decline following HIV infection. For localized proton MR spectroscopy, typical voxel placement used to evaluate PWH includes the basal ganglia, WM, and cortical GM [68]. Meta-analysis of HIV neurometabolite studies showed consistently lower total *N*-acetyl-aspartate (NAA)/total creatine (tCr), higher total choline (tCh)/tCr, and higher myoinositol (mI)/tCr ratios associated with chronic HIV infection [49]. Although many studies used tCr as a reference and reported metabolite ratios [68], HIV infection may influence tCr concentrations [69]. Hence, absolute quantification of metabolite concentrations removes the ratio confounding factor in assessment of neurochemical abnormalities. Levels of neuronal metabolites, including NAA, are lower in later stages of HAND, whereas glutamate levels are already lower in earlier stages of HAND and correlated well with cognitive deficits [70]. Levels of glial metabolites, especially mI, along with tCr and tCh, are also elevated in early stages of HAND, suggesting ongoing neuroinflammation and glial activation.

Further evidence that myoinositol and choline compounds reflect chronic neuroinflammation was shown by their correlations with  $\beta$ -amyloid tracer uptake (Pittsburgh compound B),

typically associated with neuroinflammation, in 311 cognitively normal elderly at risk for Alzheimer disease [71]. Myo-inositol levels also appeared to be more sensitive than a microglial positron emission tomography (PET) tracer (PK-11195) for detecting inflammation in patients coinfecting with HIV and hepatitis C virus [72].

## PET IMAGING

Brain PET imaging performed early in the HIV epidemic found subcortical hypermetabolism on <sup>18</sup>F-fluorodeoxyglucose (FDG) PET, interpreted as a reflection of neuroinflammation [73, 74], while hypometabolism was observed in the later stages of disease, assumed to be related to neuronal loss [75].

More recently, brain PET imaging has used various targets and ligands (Table 1) to evaluate both the neuropathophysiology of HIV and the effects of treatment and comorbid conditions, particularly cardiovascular disease [84] (Table 2) [85]. Longitudinal FDG PET demonstrated varied regional brain FDG uptake over the course of treated HIV, decreasing in subcortical structures as peripheral viral load and immune markers (interleukin 6R and soluble CD14) declined 6–8 weeks after ART while increasing in the frontal cortex, suggesting normalization of cortical dysfunction with ART initiation [78]. At 2 years after ART initiation, however, subcortical FDG uptake further decreased, suggesting that neuronal loss that may contribute to cognitive deficits [78]. Cross-sectional FDG PET imaging in well-treated chronic infection revealed lower uptake in mesial frontal and anterior cingulate cortex [79, 80], although the studies were not robustly generalizable owing to a focus

on predominantly white men with limited comorbidity. A more recent FDG study in chronically infected, virally suppressed PWH found that HIV status best predicted thalamic hypometabolism, whereas cardiovascular disease was a better

**Table 1. Positron Emission Tomography Target and Ligands Used in Human Immunodeficiency Virus Neuroimaging**

Target	Radioligand	Study Focus	References
Glucose metabolism	<sup>18</sup> F-FDG	Neuroimmune response, neuronal function	[59–62, 76, 77]
18-kDa TSPO	<sup>11</sup> C-PK11195, <sup>11</sup> C-DPA-713, <sup>18</sup> F-DPA714, <sup>11</sup> C-PBR128	Brain injury, neuroimmune response	[63–70]
Synaptic vesicle glycoprotein 2	<sup>11</sup> C-UCB-J	Synaptic integrity	[78]
Amyloid plaque	<sup>11</sup> C-PiB; <sup>18</sup> F-florbetaben, <sup>18</sup> F-AV-45 (florbetapir)	Patterns of localized or whole-brain amyloid plaque	[79–82]
Tau	<sup>18</sup> F-AV-1451 (flortaucipir)	Patterns of localized tau	[83]
Dopaminergic and serotonergic systems	<sup>11</sup> C-raclopride, <sup>18</sup> F-fallypride; <sup>11</sup> C-cocaine, <sup>18</sup> F-FP-CMT, <sup>11</sup> C-DASB	Neurotransmitter system integrity and function	[71–75, 84]

Abbreviations: FDG, fluorodeoxyglucose; TSPO, translocator protein; PiB, Pittsburgh compound B.

**Table 2. Factors Affecting Central Nervous System Measures**

HIV infection-related variables	<ul style="list-style-type: none"> <li>Degree of viral suppression</li> <li>Nadir CD4<sup>+</sup> cell count</li> <li>Current CD4<sup>+</sup> cell count</li> <li>HIV infection duration</li> <li>AIDS-defining illness history</li> </ul>
Treatment-related variables	<ul style="list-style-type: none"> <li>Time before beginning ART</li> <li>ART type</li> <li>ART adherence</li> </ul>
Systemic inflammation [86]	<ul style="list-style-type: none"> <li>Monocyte activation markers               <ul style="list-style-type: none"> <li>sCD14</li> <li>sCD163</li> <li>Lipopolysaccharide levels</li> </ul> </li> <li>Cytokines               <ul style="list-style-type: none"> <li>IP-10</li> <li>IFN-α</li> <li>IL-6</li> <li>IL-10</li> <li>IL-15</li> </ul> </li> </ul>
Comorbid conditions	<ul style="list-style-type: none"> <li>Hepatitis C</li> <li>Substance use               <ul style="list-style-type: none"> <li>Alcohol</li> <li>Marijuana</li> <li>Cocaine</li> <li>Methamphetamines</li> <li>Nicotine</li> </ul> </li> <li>Psychiatric disorders               <ul style="list-style-type: none"> <li>Anxiety</li> <li>Major depressive disorders</li> <li>Posttraumatic stress disorder</li> <li>Schizophrenia</li> </ul> </li> <li>Cerebrovascular risk               <ul style="list-style-type: none"> <li>Cigarette smoking</li> <li>Hypertension</li> <li>Diabetes</li> <li>Hyperlipidemia</li> <li>Hypercholesterolemia</li> </ul> </li> </ul>
Demographic factors	<ul style="list-style-type: none"> <li>Age</li> <li>Sex</li> <li>Socioeconomic status</li> <li>Premorbid cognitive function</li> </ul>

Abbreviations: ART, antiretroviral therapy; HIV, human immunodeficiency virus; IFN, interferon; IL-6, IL-10, and IL-15, interleukin 6, 10, and 15; IP-10, IFN-induced protein 10; sCD14, soluble CD14; sCD163, soluble CD163.

predictor of whole-brain metabolism than HIV status, suggesting an integral role of comorbid conditions, namely cardiovascular disease, in controlling brain involvement in HIV [84].

In addition to quantification of glucose metabolism, which reflects a combination of neuroinflammation and neuronal function, animal and human brain PET imaging targeted microglial activation markers [81–83, 87–91], neurotransmitter signaling systems [76, 77, 92–95], synaptic integrity [96] and pathological correlates, such as amyloid and tau deposition [97–102]. Neuroinflammation in HIV is likely due to microglial activation, peripheral monocytes infiltration, astrocytic activation, and possibly lymphocytic infiltration. To date, the most commonly pursued neuroinflammation imaging target in HIV is the 18-kDa translocator protein (TSPO), an outer mitochondrial membrane receptor expressed in resident microglia and monocyte-derived macrophages, astrocytes, endothelial cells, and choroid plexus/ependymal cells. TSPO expression is up-regulated in activated microglia, marking deviation from the normally low levels of parenchymal TSPO expression in healthy brain [103].

Human TSPO-PET imaging in PWH, however, has yielded inconsistent findings, in part likely owing to differences in radiotracer properties across first- and second-generation TSPO-targeting ligands. For example, the first-generation TSPO radiotracer <sup>11</sup>C-PK11195 is limited by low target specificity, and while 2 studies found higher TSPO brain uptake in PWH than in controls using <sup>11</sup>C-PK11195 [88, 90], another found no group differences [104]. Using a more specific, second-generation radiotracer for TSPO imaging, <sup>11</sup>C-DPA713, higher TSPO binding (distribution volume) in the WM, cingulate cortex and supramarginal gyrus relative to GM was detected in PWH relative to controls, suggesting neuroinflammatory changes [105]. Lower global TSPO expression, but higher regional tracer uptake in the parietal and occipital lobes and globus pallidus, were also observed in PWH [87]; however, another second-generation TSPO radiotracer, <sup>11</sup>C-PBR128 found no group differences [81]. Higher TSPO uptake also correlated with lower cognitive performance in PWH, although the involved regions and cognitive domains varied across studies [81, 82, 87, 88]. These conflicting results may be due to differences in cohort characteristics, ligands used, functions examined, or analysis methods.

HIV protein neurotoxicity, another postulated mechanism of CNS injury, may affect specific neurotransmitter systems, which were assessed using a variety of established PET ligands [76, 77, 92, 94, 95, 106, 107]. Lower synaptic density measured with <sup>11</sup>C-UCB-J was found in the frontostriatal-thalamic circuit and other cortical areas of older male PWH on ART compared with uninfected controls, suggesting synaptic loss [96]. Finally, studies investigating amyloid or tau accumulation as underlying causes of HAND found no increased burden of amyloid [97–99, 101] or tau protein [100] in virally suppressed PWH relative to cognitively normal controls.

## MAGNETOENCEPHALOGRAPHY

Magnetoencephalography (MEG) is another noninvasive neuroimaging technique with excellent temporal (ie, milliseconds) and spatial precision (ie, 3–5 mm). The method directly measures the minute magnetic fields that naturally emanate from electrophysiological activity in populations of neurons, with the strength of these neuromagnetic fields being proportional to the amplitude of the underlying electrical currents [108]. Almost all the MEG studies in PWH focus on virally suppressed cohorts [109].

One of the most consistent findings in PWH is elevated spontaneous cortical activity in task-related brain regions [110–115]. This activity modulates the oscillatory neural dynamics serving cognitive processing [110–115]. Spontaneous activity reflects the seemingly random neuronal discharges, fluctuations in dendritic currents, and other electrical field phenomena that occur across the cortex in the absence of exogenous and endogenous inputs. In PWH, sharply elevated spontaneous activity was shown in brain regions serving visuospatial attention [110, 114], selective attention [111], somatosensory processing [112, 113, 115], and working memory [116]. Several studies showed increased spontaneous activity that distinguishes cognitively impaired and unimpaired PWH and both HIV groups from controls [110, 111, 113]. Such elevated spontaneous cortical activity is related to both cognitive and motor processing and occurs in healthy aging [117–120], suggesting accelerated aging in PWH [121]. Interestingly, regular cannabis use may normalize elevated spontaneous cortical activity in PWH and thereby improve cortical function and cognitive performance [114].

MEG studies also showed deficits in the neural oscillatory dynamics serving early visual processing [110, 112, 122], motor function [123], selective attention [111, 124], attentional reorienting [125], visuospatial attention [122, 126], working memory [116, 127], and somatosensory processing [86, 112, 113, 115]. Frequently, these oscillatory aberrations were tightly coupled to worse cognitive performance in PWH. Several of these studies also enrolled relatively large samples and examined the impact of aging on cognitive function and the underlying oscillatory dynamics in PWH [113, 122, 124, 125]. Broadly, these MEG studies also show aberrant aging trajectories in PWH. The most recent data, however, suggest that these effects are driven by the cognitively impaired subgroup (ie, those with HIV-associated neurocognitive disorder) [125].

Neural aberrations in the visual and somatosensory cortices were reported across multiple studies focusing on different cognitive constructs (eg, visual attention). Furthermore, the available data do not support simple dichotomies such as deficits in cortical versus subcortical areas or association versus sensory cortices, as studies have found aberrations across multiple sensory regions and a broad variety of association cortices, including prefrontal and parietal attention networks. All but one MEG study focused on virally suppressed PWH [127], and

almost all MEG studies excluded participants with severe psychiatric diseases (eg, PTSD or schizophrenia), substance use disorders, and other possibly confounding conditions. Such an approach ensures that the findings are specific to HIV infection rather than confounders but limits the generalizability to PWH who have a high prevalence of these characteristics.

Work in recent studies suggests that MEG-derived cortical maps are highly reliable for  $\geq 3$  years in individual participants [128, 129], which is critical for establishing the veracity and predictive utility of MEG markers [130]. Fortunately, most active MEG sites in neuroHIV research recently installed identical instrumentation, which allows the merging of data sets across sites to build even larger samples.

### USE OF MULTIMODAL NEUROIMAGING TO INFORM RESULTS

Recognizing that changes in cognition may be on asynchronous trajectories with functional or structural brain imaging changes, combining multiple features from neuroimaging data may improve identification and tracking of functional outcomes of the HIV-associated brain injury. Novel “fusion” approaches that jointly analyze multiple neuroimaging features have the potential to reveal interrelated patterns across modalities and in spatially distinct regions beyond detection with a single modality [131]. A 2021 analysis in PWH combined T1-weighted MR imaging, DTI, and rsfMR imaging and found that lower scores on cognitive functions related to abnormal morphometry (smaller volumes of the thalamus and visual, posterior parietal, and orbitofrontal cortices), compromised WM integrity (lower FA throughout the corpus callosum and association fibers), and abnormal activity in frontoparietal and occipital networks [132]. On this identified joint component, PWH had lower loadings for both GM volume and WM integrity, suggesting that HIV-associated alterations in brain structure may contribute to cognitive impairment.

In another multiparametric study of HIV, lower FA in the corpus callosum body correlated with greater functional connectivity in linked GM regions; cognitive impairment was associated with low FA in the corpus callosum; and higher functional connectivity occurred in linked GM regions [133]. Joint analysis of MR imaging and neuropsychological data classified individuals ranging across unaffected controls, HIV without cognitive impairment, HIV with mild cognitive impairment, and HAND [134]. Machine learning algorithms using resting state networks classified individuals by HIV status and cognitive status [135]. They also showed that polysubstance use, race, educational attainment, and volumes of the precuneus, cingulate, nucleus accumbens, and thalamus differentiated membership in the normal versus impaired clusters. These emerging studies demonstrate the value of multimodal data fusion for identifying neural substrates of complex

cognitive decline, even when observations for compromise are not in temporal lockstep.

### STRATEGIC DESIGN AND ANALYTIC APPROACHES TO ACHIEVE GREATER CONSISTENCY

Given the observational nature of HIV neuroimaging data, both experimental and statistical control can increase sensitivity to detection of subtle HIV effects on brain structure and function. Potential confounds, such as comorbid conditions and variable clinical features common in PWH, raise the question of whether neuroimaging changes reported as HIV effects are related solely to viral infection [7]. Hence, some neuroimaging changes attributed to HIV might have originated from confounding effects [136–138] (Table 2).

Because PWH exhibit a wide range of demographic variations and medical comorbid conditions, larger sample sizes will facilitate the formation of stratified subgroups, which can delineate their influences on neuroimaging findings [85]. This stratification will also allow more representative, ecologically valid assessment of chronic HIV infection and its course. Across-diagnostic profile comparisons are also useful for establishing HIV-specific deficit profiles [1, 32].

In addition to cohort characteristics, variation in image acquisition and analysis techniques may contribute to study outcome heterogeneity. Current harmonization methods have reduced, but not eliminated, inconsistencies related to image acquisition and processing differences across sites [139].

#### Experimental Control

The goal of increasing sample size in HIV neuroimaging studies by pooling data across multiple sites presents challenges. In addition to the administrative overhead needed to coordinate activities among sites, adoption of standardized data acquisition systems and protocols are essential for multisite studies, because using a common scanner platform, hardware, and software (manufacturer, model, field strength, head coil, software version) across sites will minimize these variables. Maintenance of identical acquisition protocols, however, can be complicated by site hardware and software upgrades or replacement, circumstances often beyond the control of study investigators. Nevertheless, a standardized imaging protocol mitigates the risk that observed cohort differences are an artifact of acquisition differences. The Alzheimer’s Diseases Neuroimaging Initiative (ADNI), Adolescent Brain Cognitive Development Study (ABCD), and Human Connectome Project (HCP) have successfully implemented standardized protocols across multiple sites [140–142]. Examples of multisite studies in PWH include CHARTER and ENIGMA-HIV, which provide data access to the public for additional analyses [19, 143].



A first-tier, MR imaging protocol should include (1) high-resolution T1-weighted imaging for structural analysis and coregistration with other MR imaging sequences and neuroimaging modalities (eg, PET and MEG), (2) T2-weighted imaging for cerebrospinal fluid–tissue distinction, (3) FLAIR sequences for detecting WM hyperintensities, (4) a high-resolution, multishell diffusion sequence with adequate signal-to-noise for estimation of microstructural WM measures and more complex modeling of structural connectivity, (5) multiband rsfMR imaging to determine functional connectivity, and (6) ASL to assess brain perfusion. Total imaging time for these suggested first-tier sequences can be <1 hour, especially if multiband approaches are used, thus minimizing participant burden and scanner costs. These sequences also allow comparison with standing multisite studies, such as ADNI, HCP, National Consortium on Alcohol and Neurodevelopment in Adolescence, and ABCD, that have publicly available imaging data on healthy controls from preadolescence to senescence for comparison with those in PWH. Using a tiered approach, other sequences such as task functional MR imaging, quantitative susceptibility mapping, or MR spectroscopy, and other modalities (eg, MEG and PET), can be added to site protocols, depending on the research question.

Regarding MEG protocols, resting-state recordings at 1 kHz or faster are essential for assessing spontaneous activity and whole-brain connectivity, while a targeted battery of task-based paradigms would help delineate altered brain dynamics in the cognitive networks most commonly affected in PWH. Selecting a standard set of cognitive tasks with identical stimulus presentation parameters across sites and recording empty-room MEG data to compute noise covariance matrices would allow the data to be effectively coalesced with experimental rigor.

Standardizing PET studies is more challenging than MR imaging and MEG, considering the major differences in scanner models, resolutions, configurations, and reconstruction algorithms, among other site-specific parameters. In addition, multiple ligands with different characteristics (eg, lipophilicity, brain availability, affinity, specific to nonspecific binding) are often used to image the same targets (eg, TSPO). Different analysis approaches and patient populations add to the variability and discordance of PET studies. Despite the generally insurmountable differences in infrastructure and ligand availabilities across centers, reaching a unified approach to compartmental modeling and analysis methods of various ligands, especially those for neuroinflammation, may diminish protocol discordance. Future work could take advantage of novel PET imaging ligands (eg, new inflammation targets [144, 145]) and validated PET imaging ligands and reduce current limitations. Reaching a unified approach for compartmental modeling and analysis methods of target ligands, especially in neuroinflammation imaging, and a thorough assessment of current

and historical comorbid conditions in PWH would address potential confounders [144–146].

#### Quality Control

Rigorous quality control to assure limited head motion, appropriate anatomical coverage, and adherence to protocol parameters can also improve consistency. Regular scanning with structural and functional phantoms (both standardized and human phantoms) provides objective assessment of scanner drift, potential correction factors, and stability measures for across time and multisite harmonization. Thorough quality assurance is particularly important in rsfMR imaging studies, in which the changes in interregional functional connectivity are vulnerable to physiological noise from many sources, including head motion, cardiac activity and respiration [7]. Image analyses may exploit semiautomated or fully automated preprocessing pipelines that facilitate quality assurance procedures. These pipelines can simplify computational effort before statistical analysis, but different pipelines can also introduce variabilities [147–150]. Hence, a common image preprocessing approach for each modality, supported by a centralized imaging core, would decrease heterogeneity in HIV neuroimaging studies.

#### Longitudinal Designs

Although most HIV neuroimaging studies are cross-sectional, longitudinal designs are preferred in assessing ART effects on the CNS and disease progression. The repeated measures designs allow each participant to serve as their own control. Because chronic HIV samples are diverse in associated comorbid conditions, a longitudinal design provides within-subject accounting of comorbidity effects. A balanced group of HIV-seronegative controls should be included in studies to account for aging, sex, or other effects. To isolate ART effects on the CNS, investigators may assess PWH both before and after initiating ART. They may also consider statistically adjusting for the CNS penetration-effectiveness score of participants' ART regimens or the Veterans Aging Cohort Study index to estimate risk of 5-year all-cause mortality in PWH [151–153]. While longitudinal studies are preferred to answer many questions, particularly the effects of ART and aging on the CNS, they do require additional resources and comprehensive participant follow-up.

#### Statistical Control

Even with the most robust efforts to minimize site differences in acquisition protocols and equipment, residual “site” variance is likely to persist. Novel approaches to harmonize data from multiple sites (eg, ComBat [154]) may reduce inconsistencies related to image acquisition and processing differences across sites.

More problematic are the use of poorly matched control groups and the lack of adequate statistical adjustment for the

effects of various confounding factors on imaging measures. To study the effects of “uncomplicated” HIV on brain structure and function, experimental designs often eliminate or minimize confounders, which greatly limits generalizability of the results to the diverse population of PWH. Statistical approaches can adjust for nuisance variables not completely controlled experimentally. However, a large sample size will be required for such adjustments. Successful selection of covariate effects will improve statistical model fit by reducing error variance. Nuisance variables of interest include age, sex, and a range of comorbid conditions (Table 2).

One complexity encountered with this approach is that when nuisance variables exhibit collinearity, their individual contribution to the measure of interest cannot be determined. Examples include strong associations between hepatitis C virus infection and heroin use and the coupling of smoking and other cerebrovascular risk factors. Standard techniques for predictor collinearity can be used to mitigate these effects. Applications of statistical control techniques in large sample sizes afford subgroup stratification that may yield greater generalizability to the PWH population, while still accounting for commonly encountered clinical differences and comorbid conditions.

Another goal for the HIV neuroimaging community is replication of results by facilitating sharing of existing data sets. In addition to harmonized data collection and processing in future prospective studies, replications using existing data collected could be an efficient means to validate current claims that can withstand the process of out-of-sample replication. For instance, from the rapidly growing field of functional MR imaging replication, protocols with the strongest task-related activity have the best replication [155]. The widespread sharing of carefully curated data sets would also facilitate greater use by the machine learning community, and thereby lead to the emergence of new markers of HIV-related cognitive decline and potential targets for future therapeutics. Groups such as ENIGMA have started working toward this goal by pooling data sets. The next steps will include a survey of the HIV neuroimaging community to assess common sequences and numbers of participant among groups.

## CONCLUSIONS

HIV neuroimaging studies began nearly 4 decades ago with the predominant use of computed tomography for qualitative characterization of parenchymal atrophy and CNS opportunistic infections associated with AIDS. As knowledge of HIV neuropathology and treatments evolved, we now have multiple advanced imaging modalities to detect the subtle brain injury effects in treated, virally suppressed cohorts. Our next challenge is to undertake the measurement, design, and analysis complexities associated with HIV neuroimaging to achieve greater consistency in the *in vivo* characterization of HIV infection and to track its dynamic course across the life span. Critical

comorbid conditions to address include psychiatric disorders, substance use disorders, and cardiovascular risk factors. Larger samples collected with standardized acquisition protocols that include the suggested first-tier protocol will allow for pooling of data sets across sites. Rigorous experimental and statistical control methods can reduce the variability in estimates of how HIV infection *per se* affects brain structure and function. These methods include use of well-balanced control groups, adjustment for nuisance variables not completely controlled experimentally, and data harmonization techniques for multisite studies. Critically, these approaches will reveal the neuroimaging data elements best suited for identifying biotypes of CNS complications, HIV-aging interactions, and potential treatment responses in PWH.

## Notes

**Financial support.** This work was supported by the National Institutes of Health support (grants AA017347, K23 MH118070, R01 MH116782, R01 MH118013, R01 DA047828, R01 DA045565, R21NS122511, R01DA054009, R01MH118031, R01DA047149, and R01DA052827).

**Supplement sponsorship.** This article appears as part of the supplement “State of the Science of Central Nervous System Complications in People With HIV,” sponsored by the National Institutes of Health, National Institute of Mental Health.

**Potential conflicts of interest.** All authors: No reported conflicts. All authors have submitted the ICMJE Form for Disclosure of Potential Conflicts of Interest. Conflicts that the editors consider relevant to the content of the manuscript have been disclosed.

## References

1. Valcour V, Chalermchai T, Sailasuta N, et al. Central nervous system viral invasion and inflammation during acute HIV infection. *J Infect Dis* **2012**; 206:275–82.
2. Wang T, Rumbaugh Jeffrey A, Nath A. Viruses and the brain: from inflammation to dementia. *Clin Sci* **2006**; 110:393–407.
3. Adeli E, Zahr NM, Pfefferbaum A, Sullivan EV, Pohl KM. Novel machine learning identifies brain patterns distinguishing diagnostic membership of human immunodeficiency virus, alcoholism, and their comorbidity of individuals. *Biol Psychiatry Cogn Neurosci Neuroimaging* **2019**; 4:589–99.
4. Thomas Yeo BT, Sabuncu MR, Desikan R, Fischl B, Golland P. Effects of registration regularization and atlas sharpness on segmentation accuracy. *Med Image Anal* **2008**; 12:603–15.
5. Dewey J, Hana G, Russell T, et al. Reliability and validity of MRI-based automated volumetry software relative to auto-assisted manual measurement of subcortical structures in HIV-infected patients from a multisite study. *Neuroimage* **2010**; 51:1334–44.

6. O'Connor EE, Zeffiro TA, Zeffiro TA. Brain structural changes following HIV infection: meta-analysis. *AJNR Am J Neuroradiol* **2018**; 39:54–62.
7. O'Connor E, Zeffiro T. Is treated HIV infection still toxic to the brain? *Prog Mol Biol Transl Sci* **2019**; 165:259–84.
8. Sanford R, Fellows LK, Ances BM, Collins DL. Association of brain structure changes and cognitive function with combination antiretroviral therapy in HIV-positive individuals. *JAMA Neurol* **2018**; 75:72–9.
9. Kallianpur KJ, Shikuma C, Kirk GR, et al. Peripheral blood HIV DNA is associated with atrophy of cerebellar and subcortical gray matter. *Neurology* **2013**; 80:1792–9.
10. McCutchan JA, Marquie-Beck JA, Fitzsimons CA, et al. Role of obesity, metabolic variables, and diabetes in HIV-associated neurocognitive disorder. *Neurology* **2012**; 78:485–92.
11. Thompson PM, Dutton RA, Hayashi KM, et al. 3D mapping of ventricular and corpus callosum abnormalities in HIV/AIDS. *Neuroimage* **2006**; 31:12–23.
12. Thompson PM, Dutton RA, Hayashi KM, et al. Thinning of the cerebral cortex visualized in HIV/AIDS reflects CD4<sup>+</sup> T lymphocyte decline. *Proc Natl Acad Sci U S A* **2005**; 102:15647–52.
13. Clifford KM, Samboju V, Cobigo Y, et al. Progressive brain atrophy despite persistent viral suppression in HIV patients older than 60 years. *J Acquir Immune Defic Syndr* **2017**; 76:289–97.
14. Cohen RA, Harezlak J, Schifitto G, et al. Effects of nadir CD4 count and duration of human immunodeficiency virus infection on brain volumes in the highly active antiretroviral therapy era. *J Neurovirol* **2010**; 16:25–32.
15. Sanford R, Ances BM, Meyerhoff DJ, et al. Longitudinal trajectories of brain volume and cortical thickness in treated and untreated primary HIV infection. *Clin Infect Dis* **2018**; 67:1697–704.
16. Pfefferbaum A, Zahr NM, Sassoos SA, Kwon D, Pohl KM, Sullivan EV. Accelerated and premature aging characterizing regional cortical volume loss in human immunodeficiency virus infection: contributions from alcohol, substance use, and hepatitis C coinfection. *Biol Psychiatry Cogn Neurosci Neuroimaging* **2018**; 3:844–59.
17. Tesic T, Boban J, Bjelan M, Todorovic A, Kozic D, Brkic S. Basal ganglia shrinkage without remarkable hippocampal atrophy in chronic aviremic HIV-positive patients. *J Neurovirol* **2018**; 24:478–87.
18. O'Connor EE, Zeffiro T, Lopez OL, Becker JT, Zeffiro T. HIV Infection and age effects on striatal structure are additive. *J Neurovirol* **2019**; 25:480–95.
19. Nir TM, Fouche JP, Ananworanich J, et al. Association of immunosuppression and viral load with subcortical brain volume in an international sample of people living with HIV. *JAMA Netw Open* **2021**; 4:e2031190.
20. O'Connor EE, Zeffiro TA, Lopez OL, Becker JT. Differential effects of AIDS and chronic human immunodeficiency virus infection on gray matter volume. *Clin Infect Dis* **2021**; 73:e2303–10.
21. Ances BM, Ortega M, Vaida F, Heaps J, Paul R. Independent effects of HIV, aging, and HAART on brain volumetric measures. *J Acquir Immune Defic Syndr* **2012**; 59:469–77.
22. Tate DF, Sampat M, Harezlak J, et al. Regional areas and widths of the midsagittal corpus callosum among HIV-infected patients on stable antiretroviral therapies. *J Neurovirol* **2011**; 17:368–79.
23. Nichols MJ, Gates TM, Soares JR, et al. Atrophic brain signatures of mild forms of neurocognitive impairment in virally suppressed HIV infection. *AIDS* **2019**; 33:55–66.
24. Alakkas A, Ellis RJ, Watson CW, et al. White matter damage, neuroinflammation, and neuronal integrity in HAND. *J Neurovirol* **2019**; 25:32–41.
25. Jernigan TL, Archibald SL, Fennema-Notestine C, et al. Clinical factors related to brain structure in HIV: the CHARTER study. *J Neurovirol* **2011**; 17:248–57.
26. Su T, Wit FW, Caan MW, et al. White matter hyperintensities in relation to cognition in HIV-infected men with sustained suppressed viral load on combination antiretroviral therapy. *AIDS* **2016**; 30:2329–39.
27. Sanford R, Strain J, Dadar M, et al. HIV infection and cerebral small vessel disease are independently associated with brain atrophy and cognitive impairment. *AIDS* **2019**; 33:1197–205.
28. Wu M, Fatukasi O, Yang S, et al. HIV disease and diabetes interact to affect brain white matter hyperintensities and cognition. *AIDS* **2018**; 32:1803–10.
29. McMurtray A, Nakamoto B, Shikuma C, Valcour V. Small-vessel vascular disease in human immunodeficiency virus infection: the Hawaii aging with HIV cohort study. *Cerebrovasc Dis* **2007**; 24:236–41.
30. Cao B, Kong X, Kettering C, Yu P, Ragin A. Determinants of HIV-induced brain changes in three different periods of the early clinical course: a data mining analysis. *Neuroimage Clin* **2015**; 9:75–82.
31. Nir TM, Jahanshad N, Ching CRK, et al. Progressive brain atrophy in chronically infected and treated HIV+ individuals. *J Neurovirol* **2019**; 25:342–53.
32. Guha A, Brier MR, Ortega M, Westerhaus E, Nelson B, Ances BM. Topographies of cortical and subcortical volume loss in HIV and aging in the cART era. *J Acquir Immune Defic Syndr* **2016**; 73:374–83.
33. Sanford R, Fernandez Cruz AL, Scott SC, et al. Regionally specific brain volumetric and cortical thickness changes in HIV-infected patients in the HAART era. *J Acquir Immune Defic Syndr* **2017**; 74:563–70.

34. Cole JH, Underwood J, Caan MW, et al. Increased brain-predicted aging in treated HIV disease. *Neurology* **2017**; 88:1349–57.
35. Cole JH, Caan MWA, Underwood J, et al. No evidence for accelerated aging-related brain pathology in treated human immunodeficiency virus: longitudinal neuroimaging results from the Comorbidity in Relation to AIDS (COBRA) project. *Clin Infect Dis* **2018**; 66:1899–909.
36. Zahr NM, Pohl KM, Pfefferbaum A, Sullivan EV. Dissociable contributions of precuneus and cerebellum to subjective and objective neuropathy in HIV. *J Neuroimmune Pharmacol* **2019**; 14:436–47.
37. Sullivan EV, Rosenbloom MJ, Rohlfing T, Kemper CA, Deresinski S, Pfefferbaum A. Pontocerebellar contribution to postural instability and psychomotor slowing in HIV infection without dementia. *Brain Imaging Behav* **2011**; 5:12–24.
38. O'Connor EE, Jaillard A, Renard F, Zeffiro TA. Reliability of white matter microstructural changes in HIV infection: meta-analysis and confirmation. *AJNR Am J Neuroradiol* **2017**; 38:1510–9.
39. Wright PW, Heaps JM, Shimony JS, Thomas JB, Ances BM. The effects of HIV and combination antiretroviral therapy on white matter integrity. *AIDS* **2012**; 26:1501–8.
40. Wu Y, Storey P, Cohen BA, Epstein LG, Edelman RR, Ragin AB. Diffusion alterations in corpus callosum of patients with HIV. *AJNR Am J Neuroradiol* **2006**; 27:656–60.
41. Strain JF, Burdo TH, Song SK, et al. Diffusion basis spectral imaging detects ongoing brain inflammation in virologically well-controlled HIV+ patients. *J Acquir Immune Defic Syndr* **2017**; 76:423–30.
42. Chang K, Premeaux TA, Cobigo Y, et al. Plasma inflammatory biomarkers link to diffusion tensor imaging metrics in virally suppressed HIV-infected individuals. *AIDS* **2020**; 34:203–13.
43. Li S, Wu Y, Keating SM, et al. Matrix metalloproteinase levels in early HIV infection and relation to in vivo brain status. *J Neurovirol* **2013**; 19:452–60.
44. Ragin AB, Wu Y, Storey P, Cohen BA, Edelman RR, Epstein LG. Monocyte chemoattractant protein-1 correlates with subcortical brain injury in HIV infection. *Neurology* **2006**; 66:1255–7.
45. Cysique LA, Soares JR, Geng G, et al. Erratum to: White matter measures are near normal in controlled HIV infection except in those with cognitive impairment and longer HIV duration. *J Neurovirol* **2017**; 23:548–9.
46. Cysique LA, Soares JR, Geng G, et al. White matter measures are near normal in controlled HIV infection except in those with cognitive impairment and longer HIV duration. *J Neurovirol* **2017**; 23:539–47.
47. Su T, Caan MW, Wit FW, et al. White matter structure alterations in HIV-1-infected men with sustained suppression of viraemia on treatment. *AIDS* **2016**; 30:311–22.
48. Pfefferbaum A, Rosenbloom MJ, Rohlfing T, Kemper CA, Deresinski S, Sullivan EV. Frontostriatal fiber bundle compromise in HIV infection without dementia. *AIDS* **2009**; 23:1977–85.
49. Thomas JB, Brier MR, Snyder AZ, Vaida FF, Ances BM. Pathways to neurodegeneration: effects of HIV and aging on resting-state functional connectivity. *Neurology* **2013**; 80:1186–93.
50. Egbert AR, Biswal B, Karunakaran K, et al. Age and HIV effects on resting state of the brain in relationship to neurocognitive functioning. *Behav Brain Res* **2018**; 344:20–7.
51. Samboju V, Philippi CL, Chan P, et al. Structural and functional brain imaging in acute HIV. *Neuroimage Clin* **2018**; 20:327–35.
52. Chang L, Speck O, Miller EN, et al. Neural correlates of attention and working memory deficits in HIV patients. *Neurology* **2001**; 57:1001–7.
53. Ernst T, Chang L, Jovicich J, Ames N, Arnold S. Abnormal brain activation on functional MRI in cognitively asymptomatic HIV patients. *Neurology* **2002**; 59:1343–9.
54. Chang L, Tomasi D, Yakupov R, et al. Adaptation of the attention network in human immunodeficiency virus brain injury. *Ann Neurol* **2004**; 56:259–72.
55. Ernst T, Yakupov R, Nakama H, et al. Declined neural efficiency in cognitively stable human immunodeficiency virus patients. *Ann Neurol* **2009**; 65:316–25.
56. Ances BM, Vaida F, Cherner M, et al. HIV And chronic methamphetamine dependence affect cerebral blood flow. *J Neuroimmune Pharmacol* **2011**; 6:409–19.
57. Archibald SL, Jacobson MW, Fennema-Notestine C, et al. Functional interactions of HIV-infection and methamphetamine dependence during motor programming. *Psychiatry Res* **2012**; 202:46–52.
58. Meyer VJ, Little DM, Fitzgerald DA, et al. Crack cocaine use impairs anterior cingulate and prefrontal cortex function in women with HIV infection. *J Neurovirol* **2014**; 20:352–61.
59. Meade CS, Lowen SB, MacLean RR, Key MD, Lukas SE. fMRI brain activation during a delay discounting task in HIV-positive adults with and without cocaine dependence. *Psychiatry Res* **2011**; 192:167–75.
60. Connolly CG, Bischoff-Grethe A, Jordan SJ, et al. Altered functional response to risky choice in HIV infection. *PLoS One* **2014**; 9:e111583.
61. du Plessis S, Vink M, Joska JA, et al. Prefrontal cortical thinning in HIV infection is associated with impaired striatal functioning. *J Neural Transm (Vienna)* **2016**; 123:643–51.

62. Bell RP, Towe SL, Lalee Z, Huettel SA, Meade CS. Neural sensitivity to risk in adults with co-occurring HIV infection and cocaine use disorder. *Cogn Affect Behav Neurosci* **2020**; 20:859–72.
63. Chang L, Løhaugen GC, Andres T, et al. Adaptive working memory training improved brain function in human immunodeficiency virus-seropositive patients. *Ann Neurol* **2017**; 81:17–34.
64. Chang L, Ernst T, Leonido-Yee M, Speck O. Perfusion MRI detects rCBF abnormalities in early stages of HIV-cognitive motor complex. *Neurology* **2000**; 54: 389–96.
65. Ances BM, Sisti D, Vaida F, et al. Resting cerebral blood flow: a potential biomarker of the effects of HIV in the brain. *Neurology* **2009**; 73:702–8.
66. Sen S, An H, Menezes P, et al. Increased cortical cerebral blood flow in asymptomatic human immunodeficiency virus-infected subjects. *J Stroke Cerebrovasc Dis* **2016**; 25:1891–5.
67. Petersen KJ, Metcalf N, Cooley S, et al. Accelerated brain aging and cerebral blood flow reduction in persons with human immunodeficiency virus. *Clin Infect Dis* **2021**; 73:1813–21.
68. Chelala L, O'Connor EE, Barker PB, Zeffiro TA. Meta-analysis of brain metabolite differences in HIV infection. *Neuroimage Clin* **2020**; 28:102436.
69. Chang L, Ernst T, Witt MD, Ames N, Gaiefsky M, Miller E. Relationships among brain metabolites, cognitive function, and viral loads in antiretroviral-naïve HIV patients. *Neuroimage* **2002**; 17:1638–48.
70. Ernst T, Jiang CS, Nakama H, Buchthal S, Chang L. Lower brain glutamate is associated with cognitive deficits in HIV patients: a new mechanism for HIV-associated neurocognitive disorder. *J Magn Reson Imaging* **2010**; 32: 1045–53.
71. Kantarci K, Lowe V, Przybelski SA, et al. Magnetic resonance spectroscopy,  $\beta$ -amyloid load, and cognition in a population-based sample of cognitively normal older adults. *Neurology* **2011**; 77:951–8.
72. Garvey LJ, Pavese N, Ramlackhansingh A, et al. Acute HCV/HIV coinfection is associated with cognitive dysfunction and cerebral metabolite disturbance, but not increased microglial cell activation. *PLoS One* **2012**; 7: e38980.
73. Rottenberg DA, Sidtis JJ, Strother SC, et al. Abnormal cerebral glucose metabolism in HIV-1 seropositive subjects with and without dementia. *J Nucl Med* **1996**; 37: 1133–41.
74. van Gorp WG, Mandelkern MA, Gee M, et al. Cerebral metabolic dysfunction in AIDS: findings in a sample with and without dementia. *J Neuropsychiatry Clin Neurosci* **1992**; 4:280–7.
75. von Giesen HJ, Antke C, Hefter H, Wenserski F, Seitz RJ, Arendt G. Potential time course of human immunodeficiency virus type 1-associated minor motor deficits: electrophysiologic and positron emission tomography findings. *Arch Neurol* **2000**; 57:1601–7.
76. Chang L, Wang GJ, Volkow ND, et al. Decreased brain dopamine transporters are related to cognitive deficits in HIV patients with or without cocaine abuse. *Neuroimage* **2008**; 42:869–78.
77. Wang G-J, Chang L, Volkow ND, et al. Decreased brain dopaminergic transporters in HIV-associated dementia patients. *Brain* **2004**; 127:2452–8.
78. Wang Z, Manion MM, Laidlaw E, et al. Redistribution of brain glucose metabolism in people with HIV after antiretroviral therapy initiation. *AIDS* **2021**; 35:1209–19.
79. Andersen AB, Law I, Krabbe KS, et al. Cerebral FDG-PET scanning abnormalities in optimally treated HIV patients. *J Neuroinflammation* **2010**; 7:13.
80. Towgood KJ, Pitkanen M, Kulasegaram R, et al. Regional cerebral blood flow and FDG uptake in asymptomatic HIV-1 men. *Hum Brain Mapp* **2013**; 34:2484–93.
81. Boerwinkle AH, Strain JF, Burdo T, et al. Comparison of [ $^{11}\text{C}$ ]-PBR28 binding between persons living with HIV and HIV-uninfected individuals. *J Acquir Immune Defic Syndr* **2020**; 85:244–51.
82. Rubin LH, Sacktor N, Creighton J, et al. Microglial activation is inversely associated with cognition in individuals living with HIV on effective antiretroviral therapy. *AIDS* **2018**; 32:1661–7.
83. Hammoud DA, Sinharay S, Shah S, et al. Neuroinflammatory changes in relation to cerebrospinal fluid viral load in simian immunodeficiency virus encephalitis. *mBio* **2019**; 10:e00970-19.
84. Hammoud DA, Sinharay S, Steinbach S, et al. Global and regional brain hypometabolism on FDG-PET in treated HIV-infected individuals. *Neurology* **2018**; 91: e1591–601.
85. Aung HL, Alagaratnam J, Chan P, et al. Cognitive health in persons with human immunodeficiency virus: the impact of early treatment, comorbidities, and aging. *J Infect Dis* **2023**; 227(Suppl 1):S38–47.
86. Wilson TW, Heinrichs-Graham E, Becker KM, et al. Multimodal neuroimaging evidence of alterations in cortical structure and function in HIV-infected older adults. *Hum Brain Mapp* **2015**; 36:897–910.
87. Vera JH, Guo Q, Cole JH, et al. Neuroinflammation in treated HIV-positive individuals: a TSPO PET study. *Neurology* **2016**; 86:1425–32.
88. Garvey LJ, Pavese N, Politis M, et al. Increased microglia activation in neurologically asymptomatic HIV-infected patients receiving effective ART. *AIDS* **2014**; 28:67–72.

89. Coughlin JM, Wang Y, Ma S, et al. Regional brain distribution of translocator protein using [(11)C]DPA-713 PET in individuals infected with HIV. *J Neurovirol* **2014**; 20:219–32.
90. Hammoud DA, Endres CJ, Chander AR, et al. Imaging glial cell activation with [<sup>11</sup>C]-R-PK11195 in patients with AIDS. *J Neurovirol* **2005**; 11:346–55.
91. Mankowski JL, Queen SE, Tarwater PJ, Adams RJ, Guilarte TR. Elevated peripheral benzodiazepine receptor expression in simian immunodeficiency virus encephalitis. *J Neurovirol* **2003**; 9:94–100.
92. Shah S, Sinharay S, Matsuda K, et al. Potential mechanism for HIV-associated depression: upregulation of serotonin transporters in SIV-infected macaques detected by 11C-DASB PET. *Front Psychiatry* **2019**; 10:362.
93. Sinharay S, Lee D, Shah S, et al. Cross-sectional and longitudinal small animal PET shows pre and post-synaptic striatal dopaminergic deficits in an animal model of HIV. *Nucl Med Biol* **2017**; 55:27–33.
94. Lee DE, Reid WC, Ibrahim WG, et al. Imaging dopaminergic dysfunction as a surrogate marker of neuropathology in a small-animal model of HIV. *Mol Imaging* **2014**; 13:1–10.
95. Hammoud DA, Endres CJ, Hammond E, et al. Imaging serotonergic transmission with [<sup>11</sup>C]DASB-PET in depressed and non-depressed patients infected with HIV. *Neuroimage* **2010**; 49:2588–95.
96. Weiss JJ, Calvi R, Naganawa M, et al. Preliminary in vivo evidence of reduced synaptic density in human immunodeficiency virus (HIV) despite antiretroviral therapy. *Clin Infect Dis* **2021**; 73:1404–11.
97. Vera JH, Eftychiou N, Schuerer M, et al. Clinical utility of β-amyloid PET imaging in people living with HIV with cognitive symptoms. *J Acquir Immune Defic Syndr* **2021**; 87:826–33.
98. Mohamed M, Skolasky RL, Zhou Y, et al. Beta-amyloid (Aβ) uptake by PET imaging in older HIV+ and HIV- individuals. *J Neurovirol* **2020**; 26:382–90.
99. Howdle GC, Quidé Y, Kassem MS, et al. Brain amyloid in virally suppressed HIV-associated neurocognitive disorder. *Neurol Neuroimmunol Neuroinflamm* **2020**; 7:e739.
100. Cooley SA, Strain JF, Beaumont H, et al. Tau positron emission tomography binding is not elevated in HIV-infected individuals. *J Infect Dis* **2019**; 220:68–72.
101. Ances BM, Benzinger TL, Christensen JJ, et al. <sup>11</sup>C-PiB Imaging of human immunodeficiency virus-associated neurocognitive disorder. *Arch Neurol* **2012**; 69:72–7.
102. Sinharay S, Hammoud DA. Brain PET imaging: value for understanding the pathophysiology of HIV-associated neurocognitive disorder (HAND). *Curr HIV/AIDS Rep* **2019**; 16:66–75.
103. Hammoud DA. Molecular imaging of inflammation: current status. *J Nucl Med* **2016**; 57:1161–5.
104. Wiley CA, Lopresti BJ, Becker JT, et al. Positron emission tomography imaging of peripheral benzodiazepine receptor binding in human immunodeficiency virus-infected subjects with and without cognitive impairment. *J Neurovirol* **2006**; 12:262–71.
105. Coughlin JM, Wang Y, Ma S, et al. Regional brain distribution of translocator protein using [<sup>11</sup>C] DPA-713 PET in individuals infected with HIV. *J Neurovirol* **2014**; 20:219–32.
106. Cawthorne C, Maguire P, Mercier J, et al. Human biodistribution and dosimetry of [<sup>11</sup>C]-UCB-J, a PET radiotracer for imaging synaptic density. *EJNMMI Phys* **2021**; 8:37.
107. Naganawa M, Li S, Nabulsi N, et al. First-in-human evaluation of <sup>18</sup>F-SynVesT-1, a radioligand for PET imaging of synaptic vesicle glycoprotein 2A. *J Nucl Med* **2021**; 62:561–7.
108. Wilson TW, Heinrichs-Graham E, Proskovec AL, McDermott TJ. Neuroimaging with magnetoencephalography: a dynamic view of brain pathophysiology. *Transl Res* **2016**; 175:17–36.
109. Wilson TW, Lew BJ, Spooner RK, Rezich MT, Wiesman AI. Aberrant brain dynamics in neuroHIV: evidence from magnetoencephalographic (MEG) imaging. *Prog Mol Biol Transl Sci* **2019**; 165:285–320.
110. Wiesman AI, O'Neill J, Mills MS, et al. Aberrant occipital dynamics differentiate HIV-infected patients with and without cognitive impairment. *Brain* **2018**; 141:1678–90.
111. Lew BJ, McDermott TJ, Wiesman AI, et al. Neural dynamics of selective attention deficits in HIV-associated neurocognitive disorder. *Neurology* **2018**; 91:e1860–9.
112. Spooner RK, Wiesman AI, Mills MS, et al. Aberrant oscillatory dynamics during somatosensory processing in HIV-infected adults. *Neuroimage Clin* **2018**; 20:85–91.
113. Spooner RK, Wiesman AI, O'Neill J, et al. Prefrontal gating of sensory input differentiates cognitively impaired and unimpaired aging adults with HIV. *Brain Commun* **2020**; 2:fcaa080.
114. Christopher-Hayes NJ, Lew BJ, Wiesman AI, et al. Cannabis use impacts pre-stimulus neural activity in the visual cortices of people with HIV. *Hum Brain Mapp* **2021**; 42:5446–57.
115. Casagrande CC, Lew BJ, Taylor BK, et al. Impact of HIV-infection on human somatosensory processing, spontaneous cortical activity, and cortical thickness: a multimodal neuroimaging approach. *Hum Brain Mapp* **2021**; 42:2851–61.
116. Wilson TW, Proskovec AL, Heinrichs-Graham E, et al. Aberrant neuronal dynamics during working memory operations in the aging HIV-infected brain. *Sci Rep* **2017**; 7:41568.

117. Heinrichs-Graham E, Wilson TW. Is an absolute level of cortical beta suppression required for proper movement? magnetoencephalographic evidence from healthy aging. *Neuroimage* **2016**; 134:514–21.
118. Wilson TW, Heinrichs-Graham E, Becker KM. Circadian modulation of motor-related beta oscillatory responses. *Neuroimage* **2014**; 102:531–9.
119. McDermott TJ, Wiesman AI, Mills MS, et al. tDCS modulates behavioral performance and the neural oscillatory dynamics serving visual selective attention. *Hum Brain Mapp* **2019**; 40:729–40.
120. Wiesman AI, Mills MS, McDermott TJ, Spooner RK, Coolidge NM, Wilson TW. Polarity-dependent modulation of multi-spectral neuronal activity by transcranial direct current stimulation. *Cortex* **2018**; 108:222–33.
121. Lew BJ, Schantell MD, O'Neill J, et al. Reductions in gray matter linked to epigenetic HIV-associated accelerated aging. *Cereb Cortex* **2021**; 31:3752–63.
122. Groff BR, Wiesman AI, Rezich MT, et al. Age-related visual dynamics in HIV-infected adults with cognitive impairment. *Neurol Neuroimmunol Neuroinflamm* **2020**; 7:e690.
123. Wilson TW, Heinrichs-Graham E, Robertson KR, et al. Functional brain abnormalities during finger-tapping in HIV-infected older adults: a magnetoencephalography study. *J Neuroimmune Pharmacol* **2013**; 8:965–74.
124. Lew BJ, O'Neill J, Rezich MT, et al. Interactive effects of HIV and ageing on neural oscillations: independence from neuropsychological performance. *Brain Commun* **2020**; 2:fcaa015.
125. Arif Y, Wiesman AI, O'Neill J, et al. The age-related trajectory of visual attention neural function is altered in adults living with HIV: a cross-sectional MEG study. *EBioMedicine* **2020**; 61:103065.
126. Becker KM, Heinrichs-Graham E, Fox HS, et al. Decreased MEG beta oscillations in HIV-infected older adults during the resting state. *J Neurovirol* **2013**; 19:586–94.
127. Becker JT, Cuesta P, Fabrizio M, et al. Brain structural and functional recovery following initiation of combination antiretroviral therapy. *J Neurovirol* **2012**; 18:423–7.
128. McCusker MC, Lew BJ, Wilson TW. Three-year reliability of MEG visual and somatosensory responses. *Cereb Cortex* **2021**; 31:2534–48.
129. Lew BJ, Fitzgerald EE, Ott LR, Penhale SH, Wilson TW. Three-year reliability of MEG resting-state oscillatory power. *Neuroimage* **2021**; 243:118516.
130. Becker JT, Fabrizio M, Sudre G, et al. Potential utility of resting-state magnetoencephalography as a biomarker of CNS abnormality in HIV disease. *J Neurosci Methods* **2012**; 206:176–82.
131. Calhoun VD, Sui J. Multimodal fusion of brain imaging data: a key to finding the missing link(s) in complex mental illness. *Biol Psychiatry Cogn Neurosci Neuroimaging* **2016**; 1:230–44.
132. Sui J, Li X, Bell RP, et al. Structural and functional brain abnormalities in human immunodeficiency virus disease revealed by multimodal magnetic resonance imaging fusion: association with cognitive function. *Clin Infect Dis* **2021**; 73:e2287–93.
133. Hall SA, Bell RP, Davis SW, Towe SL, Ikner TP, Meade CS. Human immunodeficiency virus-related decreases in corpus callosal integrity and corresponding increases in functional connectivity. *Hum Brain Mapp* **2021**; 42:4958–72.
134. Zhang J, Zhao Q, Adeli E, et al. Multi-label, multi-domain learning identifies compounding effects of HIV and cognitive impairment. *Med Image Anal* **2022**; 75:102246.
135. Luckett PH, Paul RH, Hannon K, et al. Modeling the effects of HIV and aging on resting-state networks using machine learning. *J Acquir Immune Defic Syndr* **2021**; 88:414–9.
136. Glans M, Cooley SA, Vaida F, et al. Effects of Framingham 10-year cardiovascular risk score and viral load on brain integrity in persons with HIV. *J Acquir Immune Defic Syndr* **2022**; 90:79–87.
137. Chow FC, Callen A, Arechiga V, Saloner D, Narvid J, Hsue PY. Intracranial vascular imaging detects arterial wall abnormalities in persons with treated HIV infection. *AIDS* **2022**; 36:69–73.
138. Kilgore CB, Strain JF, Nelson B, et al. Cardiorespiratory fitness is associated with better white matter integrity in persons living with HIV. *J Acquir Immune Defic Syndr* **2021**; 89:558–65.
139. Mukerji SS, Petersen KJ, Pohl KM, et al. Machine learning approaches to understand cognitive phenotypes in people with HIV. *J Infect Dis* **2023**; 227(Suppl 1):S48–57.
140. Weiner MW, Aisen PS, Jack CR Jr, et al. The Alzheimer's Disease Neuroimaging Initiative: progress report and future plans. *Alzheimers Dement* **2010**; 6:202–11.e7.
141. Casey BJ, Cannonier T, Conley MI, et al. The Adolescent Brain Cognitive Development (ABCD) study: imaging acquisition across 21 sites. *Dev Cogn Neurosci* **2018**; 32:43–54.
142. Van Essen DC, Ugurbil K, Auerbach E, et al. The Human Connectome Project: a data acquisition perspective. *Neuroimage* **2012**; 62:2222–31.
143. Saloner R, Heaton RK, Campbell LM, et al. Effects of comorbidity burden and age on brain integrity in HIV. *AIDS* **2019**; 33:1175–85.
144. Horti AG, Naik R, Foss CA, et al. PET imaging of microglia by targeting macrophage colony-stimulating factor 1

- receptor (CSF1R). *Proc Natl Acad Sci U S A* **2019**; 116:1686–91.
145. Shrestha S, Kim MJ, Eldridge M, et al. PET Measurement of cyclooxygenase-2 using a novel radioligand: upregulation in primate neuroinflammation and first-in-human study. *J Neuroinflammation* **2020**; 17:140.
146. Owen DR, Yeo AJ, Gunn RN, et al. An 18-kDa translocator protein (TSPO) polymorphism explains differences in binding affinity of the PET radioligand PBR28. *J Cereb Blood Flow Metab* **2012**; 32:1–5.
147. Bhagwat N, Barry A, Dickie EW, et al. Understanding the impact of preprocessing pipelines on neuroimaging cortical surface analyses. *Gigascience* **2021**; 10:giaa155.
148. Vergara VM, Mayer AR, Damaraju E, Calhoun VD. The effect of preprocessing in dynamic functional network connectivity used to classify mild traumatic brain injury. *Brain Behav* **2017**; 7:e00809.
149. Vergara VM, Mayer AR, Damaraju E, Hutchison K, Calhoun VD. The effect of preprocessing pipelines in subject classification and detection of abnormal resting state functional network connectivity using group ICA. *Neuroimage* **2017**; 145:365–76.
150. Norgaard M, Ganz M, Svarer C, et al. Optimization of preprocessing strategies in positron emission tomography (PET) neuroimaging: a [<sup>11</sup>C]DASB PET study. *Neuroimage* **2019**; 199:466–79.
151. Letendre S, Marquie-Beck J, Capparelli E, et al. Validation of the CNS penetration-effectiveness rank for quantifying antiretroviral penetration into the central nervous system. *Arch Neurol* **2008**; 65:65–70.
152. Bebu I, Tate J, Rimland D, et al. The VACS index predicts mortality in a young, healthy HIV population starting highly active antiretroviral therapy. *J Acquir Immune Defic Syndr* **2014**; 65:226–30.
153. Brown ST, Tate JP, Kyriakides TC, et al. The VACS index accurately predicts mortality and treatment response among multi-drug resistant HIV infected patients participating in the Options in Management with Antiretrovirals (OPTIMA) study. *PLoS One* **2014**; 9:e92606.
154. Fortin JP, Cullen N, Sheline YI, et al. Harmonization of cortical thickness measurements across scanners and sites. *Neuroimage* **2018**; 167:104–20.
155. Kampa M, Schick A, Sebastian A, et al. Replication of fMRI group activations in the neuroimaging battery for the Mainz Resilience Project (MARP). *Neuroimage* **2020**; 204:116223.